Journal of Materials Chemistry C

PAPER

View Article Online
View Journal | View Issue

A dual-wavelength surface-emitting distributed feedback laser from a holographic grating with an organic semiconducting gain and a doped dye

Cite this: J. Mater. Chem. C, 2014, 2, 6177

Zhihui Diao,[ab] Li Xuan,*[a] Lijuan Liu,[ab] Mingliang Xia,[c] Lifa Hu,[a] Yonggang Liu[a] and Ji Ma*[ad]

Received 16th March 2014
Accepted 27th May 2014

DOI: 10.1039/c4tc00519h

www.rsc.org/MaterialsC

An organic dual-wavelength surface-emitting distributed feedback (DFB) laser based on a waveguide configuration containing a holographic photo-curable polymer/liquid crystal (LC) periodic structure and two laser gain media is reported for the first time. In such a laser configuration, a laser dye [4-(dicyanomethylene)-2-methyl-6-(*p*-dimethylaminostyryl)-4*H*-pyran, DCM]-doped polymer/LC periodic grating was formed on the top of a semiconducting laser gain [poly(2-methoxy-5-(2′-ethyl-hexyloxy)-*p*-phenylenevinylene), MEH-PPV] layer. A dual-wavelength laser emission at 627.8 nm and 606.6 nm was obtained from the two different laser gain media. The working mechanism of the two lasing behaviors and the methods to modulate lasing wavelength positions are elaborated and demonstrated, which shows the potential to extend the applications of organic lasers.

1. Introduction

Recently, dual-wavelength lasers (DWLs) have exhibited potential for various applications, such as laser spectroscopy, nonlinear optics, THz frequency generators and medical equipment.[1] Also, DWLs are the key elements in optical communications and dual-wavelength interferometry.[2] Previous reports on DWLs are mainly achieved by Nd-doped crystals[3] or inorganic semiconducting materials.[4] For Nd-doped crystal DWLs, additional optical elements (*e.g.* mirrors) are needed to establish laser cavities, which induce optical instability and a bulky configuration. For inorganic semiconducting DWLs, the sensitivity of laser performance on the environment or rigid structure[5] limits their practical applications. On the other hand, organic gain materials, including laser dyes and organic semiconducting media, are very attractive for laser applications by virtue of their simple process, plain structure, chemically tunable emission spectrum and mechanical flexibility.[6]

We have demonstrated an organic dual-wavelength distributed feedback (DFB) laser that was achieved based on a dye [4-(dicyanomethylene)-2-methyl-6-(*p*-dimethylaminostyryl)-4*H*-pyran, DCM]-doped holographic polymer dispersed liquid crystal (HPDLC) grating with a periodic structure.[7] HPDLC is formed by photopolymerization-induced phase separation[8–11] of the liquid crystal (LC) from a photo-curable syrup under holographic exposure, while the HPDLC laser has demonstrated that it can be easily modulated by external fields such as an electric field.[12] Simultaneous laser emission with two different wavelengths *via* different Bragg orders was obtained at the edge of the sample.[7] The edge emission produced a highly diverging and inhomogeneous beam, due to a small waveguide aperture and poor facet quality. The high Bragg orders utilized in the DFB structure would result in high thresholds for both lasers.[13]

In this paper, we propose a dual-wavelength surface-emitting DFB laser from a holographic grating based on two organic gain materials. A DCM-doped HPDLC grating was formed on the top of an organic semiconductor poly(2-methoxy-5-(2′-ethyl-hexyloxy)-*p*-phenylenevinylene) (MEH-PPV) layer. The grating periodic structure was to provide the feedback for MEH-PPV and DCM *via* second Bragg order simultaneously, resulting in a coupled dual-wavelength lasing output at one direction on the sample surface. A dual-wavelength emission at 627.8 nm and 606.6 nm was generated by MEH-PPV and DCM respectively but in one laser beam. Compared with the dual-wavelength emission from a pure dye-doped HPDLC grating,[7] a dramatic reduction of the thresholds for both lasers was obtained as in the current design only second Bragg order DFB was used. Moreover, through revealing the working mechanism of the two lasing behaviors, the methods to modulate the lasing wavelength positions were demonstrated. We believe that this novel dual-wavelength surface-emitting DFB laser with photo-curable materials, a simple working mechanism and ease of laser modulation capabilities will extend the applications of organic lasers.

[a]State Key Laboratory of Applied Optics, Changchun Institute of Optics, Fine Mechanics and Physics, Chinese Academy of Sciences, Changchun, 130033, China. E-mail: xuanli@ciomp.ac.cn

[b]University of Chinese Academy of Sciences, Beijing, 100049, China

[c]Jiangsu Key Laboratory of Medical Optics, Suzhou Institute of Biomedical Engineering and Technology, Chinese Academy of Sciences, Suzhou, 215163, China

[d]Liquid Crystal Institute, Kent State University, Ohio, 44240, USA. E-mail: jma2@kent.edu

2. Experimental

The schematic structure of the proposed dual-wavelength DFB laser configuration, the experimental optical setup and a typical grating image are shown in Fig. 1. A film of an organic semiconducting MEH-PPV layer (average molecular weight 120 000; OLED Material Tech.) was spin-coated on the glass substrate in a xylene solution (6 mg mL^{-1}). The film thickness was controlled by the rotation speed. By combining the MEH-PPV coated glass substrate with a bare glass substrate, which are separated by a 6 μm Mylar spacer, an empty cell was formed. The HPDLC pre-polymer syrup was then injected into the cell. The syrup consisted of photosensitive monomers (54.6 wt%), nematic LC TEB30A (n_o = 1.522, Δn = 0.170, Slichem, 33.0 wt%), photoinitiator Rose Bengal (RB, Aldrich, 0.5 wt%), co-initiator *N*-phenylglycine (NPG, Aldrich, 1.8 wt%), chain extender *N*-vinylpyrrolidone (NVP, Aldrich, 9.1 wt%) and laser dye DCM (Aldrich, 1.0 wt%). To check the effect of refractive index, two groups of monomers were adopted in our experiments: dipentaerythritol hydroxyl pentaacrylate (DPHPA, Aldrich)/phthalic diglycol diacrylate (PDDA, Eastern Acrylic Chem.) and DPHPA/bisphenol F ethoxylate (2 EO/phenol) diacrylate (BPFEDA, Aldrich), at a weight ratio of 1 : 1. They formed DCM-doped HPDLC gratings with average refractive indices at 1.541 (DPHPA/PDDA) and 1.555 (DPHPA/BPFEDA) respectively, confirmed by using an Abbe refractometer (2WA, Kernco).

After being injected into the cell, the pre-polymer syrup underwent holographic photo-curing by two coherent *s*-polarized laser beams (9 mW cm^{-2}) at a specific angle from a 532 nm Nd:YAG laser. Then a hologram formation of alternating polymer and LC-rich layers was achieved after exposure for 5 minutes. The period of the DCM-doped HPDLC grating was carefully chosen at 394.9 nm, so that the grating could provide feedback *via* the second Bragg order for the gain materials MEH-PPV and DCM for surface emission. Fig. 1c shows the atomic force microscopy (AFM, Nanosurf) image of the sample with grating period at 394.9 nm. The sample cured by the holographic optical interference field was then pumped at 532 nm by a pulsed Nd:YAG laser (pulse duration: 8 ns; repetition rate: 3 Hz). The pump beam was focused by a cylindrical lens and incident onto the sample at an angle of 60° with respect to the glass substrate. An adjustable slit was used to select only the central portion of the pump beam with dimensions of 3 mm by 0.1 mm. The dual-wavelength laser emission was collected normal to the sample surface by using a fiber-coupled spectrometer with a resolution of 0.25 nm. A polarizer was placed between the sample and the fiber detector to verify the emitted laser polarization.

Different samples were prepared, as shown in Table 1. For sample 1a, the average refractive index of the DCM-doped HPDLC grating was 1.541 and the thickness of the MEH-PPV film was 80 nm. The period of the grating was chosen at 394.9 nm. Sample 1b had the same parameters as sample 1a but there was no DCM doped in the grating. Compared with sample 1a, the thickness of the MEH-PPV film was decreased to 70 nm in sample 2a and the average refractive index of the DCM-doped grating was changed to 1.555 in sample 3a due to a different polymer composite used. For samples 4a–4c, the periods of the grating were chosen at 390.8 nm, 399.5 nm and 403.4 nm, respectively.

Table 1 Parameters of different samples

Sample	Average refractive index of HPDLC	Thickness of MEH-PPV (nm)	Period of HPDLC (nm)
1a	1.541	80	394.9
1b[a]	1.541	80	394.9
2a	1.541	70	394.9
3a	1.555	80	394.9
4a	1.541	80	390.8
4b	1.541	80	399.5
4c	1.541	80	403.4

[a] No DCM doped in the grating.

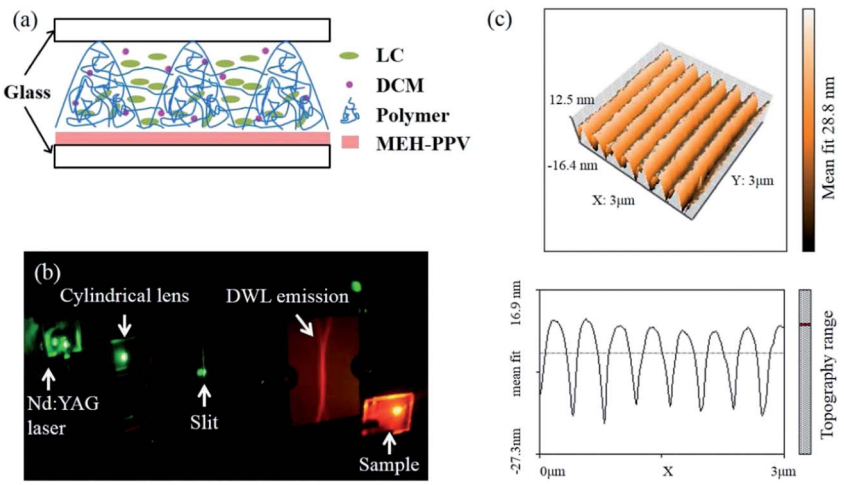

Fig. 1 (a) Schematic structure of the proposed dual-wavelength DFB laser configuration, (b) optical setup and (c) AFM image of the sample with a grating period at 394.9 nm.

3. Results and discussion

When excited above the threshold, dual-wavelength lasers were emitted at the normal to the glass substrate surface from the samples. As expected for the one-dimensional second-order DFB resonator,[14] the laser emission pattern was only confined in one direction perpendicular to the grating lines [Fig. 1(b)]. The spectra of the dual-wavelength laser of 1a were measured at a pump energy of 0.75 μJ, as shown in Fig. 2(a). Two lasers with different wavelengths located at 627.8 nm and 606.6 nm were obtained in one laser beam, and their spectral widths (full width at half maximum, FWHM) were 0.6 nm and 0.3 nm. To distinguish the sources of the two lasers, another sample (1b) with the same parameters but no DCM in the grating was tested. The lasing spectrum of 1b is shown in Fig. 2(b). It can be seen that only the 627.8 nm laser was found even at a higher pump energy of 2.0 μJ, which indicates that the MEH-PPV laser gain layer induces the 627.8 nm laser and the DCM laser dye leads to the 606.6 nm laser.

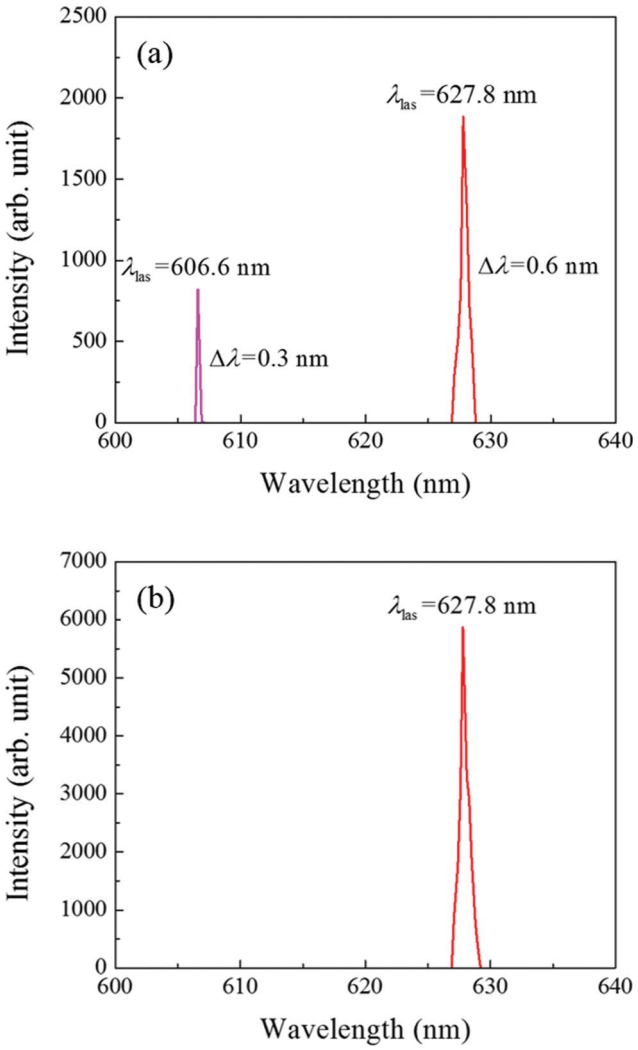

Fig. 2 Lasing spectra of (a) a dual-wavelength laser in 1a at 0.75 μJ and (b) single-wavelength in 1b without a DCM-doped grating at 2.0 μJ.

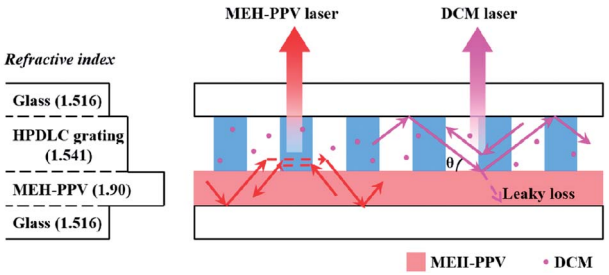

Fig. 3 Lasing mechanism of the proposed dual-wavelength DFB laser. Red solid line: lights from MEH-PPV; red dashed line: evanescent wave; pink solid line: light from DCM; pink dashed line: leaky loss.

The polarization of the dual-wavelength laser emission was detected by rotating the polarizer between the sample and the fiber detector. It showed that the two lasers were both TE polarized waves. The lasing mechanism of the 627.8 nm laser generated from MEH-PPV can be explained by the waveguide theory.[10] As shown in Fig. 3, the HPDLC grating/MEH-PPV/glass configuration defines a typical asymmetric slab waveguide, in which the HPDLC grating acts as an external feedback structure in the cladding layer. The light undergoes stimulated amplification when propagating in the MEH-PPV layer (red solid line) and also obtains feedback for specific wavelength by spreading into the grating layer near the interface as the evanescent wave form (red dashed line). The specific wavelength, *i.e.*, the laser wavelength λ_{las} follows the Bragg equation:[15]

$$\lambda_{las} = 2n_{eff}\Lambda/m, \quad (1)$$

where Λ is the grating period, m is the Bragg order and n_{eff} is the effective refractive index of the laser mode. Using $\Lambda = 394.9$ nm in our grating and $m = 2$, the effective refractive index of the 627.8 nm laser is calculated to be 1.590. In 1a, the average refractive index of the DCM-doped HPDLC grating, the refractive index of the MEH-PPV film and the refractive index of the glass substrate for the TE light are 1.541, 1.90 (ref. 16) and 1.516, respectively. According to the waveguide equation,[17] the effective refractive index of the 627.8 nm TE light in the 80 nm core layer (MEH-PPV) is 1.594. Considering polymer shrinkage during the HPDLC grating formation process, the agreement between the experimental results and theoretical calculations is good, which further proves that the 627.8 nm laser is from MEH-PPV by the asymmetric slab waveguide effect.

While for the 606.6 nm DCM laser, the working mechanism is different. As shown in Fig. 3, in the configuration of glass/grating/MEH-PPV, since the average refractive index of the core (DCM-doped grating) is lower than one of the cladding layer (MEH-PPV layer), it forms a so-called "leaky mode" slab waveguide.[18] In such a waveguide, the light in the grating layer (pink solid line) will leak into the MEH-PPV layer (pink dashed line) since there is no total reflection at the grating/MEH-PPV interface. Despite the leaky loss, a significant confinement of the light would still exist in the core layer (grating) because of the high reflectivity occurring at the grazing incidence.[18] When the gain from DCM exceeds the leaky loss, the light can propagate

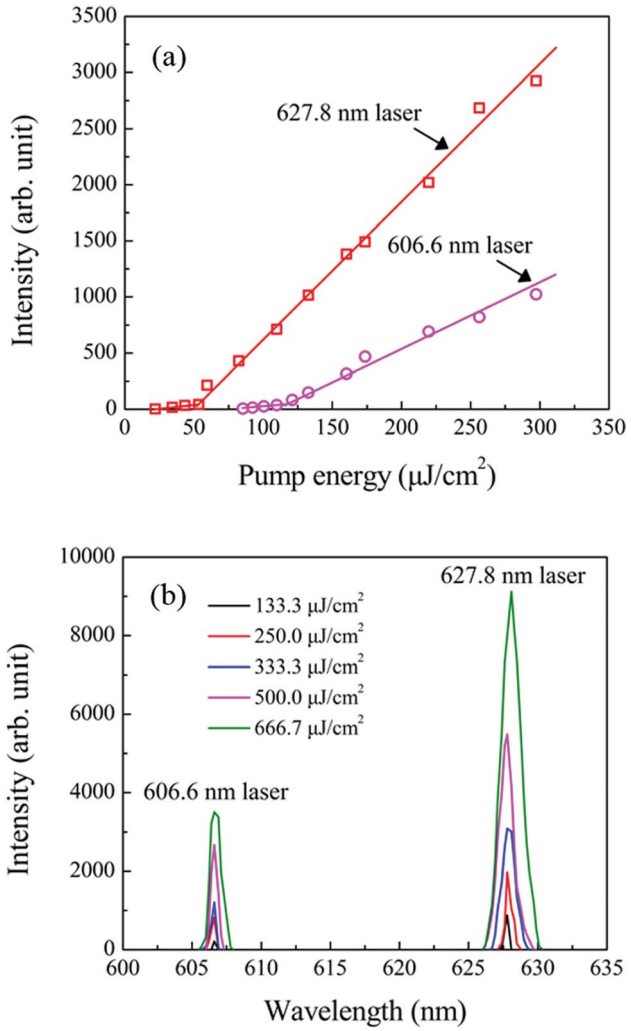

Fig. 4 (a) Laser intensity and (b) lasing spectra *versus* pump energy (1a).

in the grating layer as discrete modes and undergo stimulated amplification by obtaining feedback from the periodic grating structure. In these modes, the light will preferentially be amplified in the fundamental one that has the lowest leaky loss, showing a strong self-mode restriction capability.[19] Due to this effect, we do not observe the multi-mode laser behaviors at low pump energy (<2.0 μJ) in our experiment. According to eqn (1), the calculated effective refractive index of the 606.6 nm laser is 1.536. Compared to the average refractive index of the DCM-doped grating 1.541, we can know that the 606.6 nm laser mode propagates in the grating layer at a grazing angle θ (Fig. 3) of 4.6° [θ = arcos(1.536/1.541)]. If we put this grazing angle into the Fresnel law,[20] we can get the calculated reflectivity at the grating/MEH-PPV interface of 64.2% for the TE light and 50.8% for the TM light, which also means that the leaky loss is less for TE light, and it is the reason that the 606.6 nm laser is TE polarized at low pump energy.

Fig. 4 shows the dependence of the dual-wavelength laser intensity and lasing spectra on the pump energy of 1a. For each laser, a clear pump threshold can be obtained by an abrupt increase in the slope of curves and the output lasing intensity increases linearly as the pump energy increases beyond the pump threshold. The lasing properties of the two lasers can be well maintained in single mode lasing action, in which the changes of the spectral widths were only 1.5 nm for the MEH-PPV laser and 0.7 nm for the DCM laser when the pump energy was modulated from 0.4 μJ to 2.0 μJ (Fig. 4(b)). The threshold is 0.16 μJ (*i.e.*, pump energy density 0.053 mJ cm^{-2} or peak power density per pump laser pulse 6.7 kW cm^{-2}, the same as below) for the 627.8 nm MEH-PPV laser and 0.36 μJ (0.12 mJ cm^{-2} or 15.0 kW cm^{-2}) for the 606.6 nm DCM laser. Compared with the dual-wavelength DFB laser form the pure DCM-doped HPDLC grating *via* seventh and eighth Bragg orders with thresholds[7] of 53.20 μJ (5.32 mJ cm^{-2} or 665.0 kW cm^{-2}) and 95.44 μJ (9.54 mJ cm^{-2} or 1192.5 kW cm^{-2}), a dramatic reduction of the laser thresholds was achieved in this work. This result can be understood due to the following effects. One is from the second Bragg order used for both lasers because the lower Bragg order can reduce the threshold effectively. For the MEH-PPV laser, we ascribe the lower threshold to its higher absorption from the pump source. The absorption of the 80 nm MEH-PPV layer and 6 μm DCM-doped HPDLC grating film was 70% and 18% respectively, checked using an absorption spectrometer. So the higher absorption for the pump energy in the MEH-PPV material gives rise to a higher effective gain and a lower threshold for the 627.8 nm laser. For the DCM laser, the output lasing wavelength position is critical. The wavelength of the second order laser at 606.6 nm is located near the center of the DCM gain spectrum.[7] The laser threshold will decrease significantly when the emission wavelength moves from the edge of the gain spectrum to the center, because of the higher gain and lower re-absorption effect.[21]

Furthermore, to modulate the dual-wavelength lasing positions, the effects on the MEH-PPV semiconducting layer thickness, the average refractive index of the grating, the period of the grating and temperature were investigated. Fig. 5 shows the lasing spectra of other samples (2a–4c). When the MEH-PPV film thickness was decreased from 80 nm to 70 nm (2a), the MEH-PPV laser was shifted to 626.0 nm and the 606.6 nm DCM laser remained still, as shown in Fig. 5(a). When the average refractive index of the HPDLC grating was changed from 1.541 to 1.555 (3a), both lasers were shifted to 611.7 nm and 633.1 nm, as shown in Fig. 5(b). When the period of the grating was changed to 390.8 nm, 399.5 nm and 403.4 nm (4a–4c), the lasing wavelength positions were accordingly modulated, as shown in Fig. 5(c) and (d). For 1a, when the temperature was changed from 23 °C to 100 °C, the wavelengths for both lasers were blue-shifted, as shown in Fig. 5(e) and (f), which was attributed to the decrease of the average refractive index of the HPDLC grating because the refractive indices of the LC and the polymer would decrease with increasing temperature.[22] Since LCs can be easily aligned or re-orientated by external stimuli such as electrical, mechanical or optical force,[23] combining our results, we can conclude that the output wavelengths of the two lasers can be adjusted by changing the device parameters including the average refractive index of the grating, layer thickness and grating period or external stimuli. More meaningfully, it

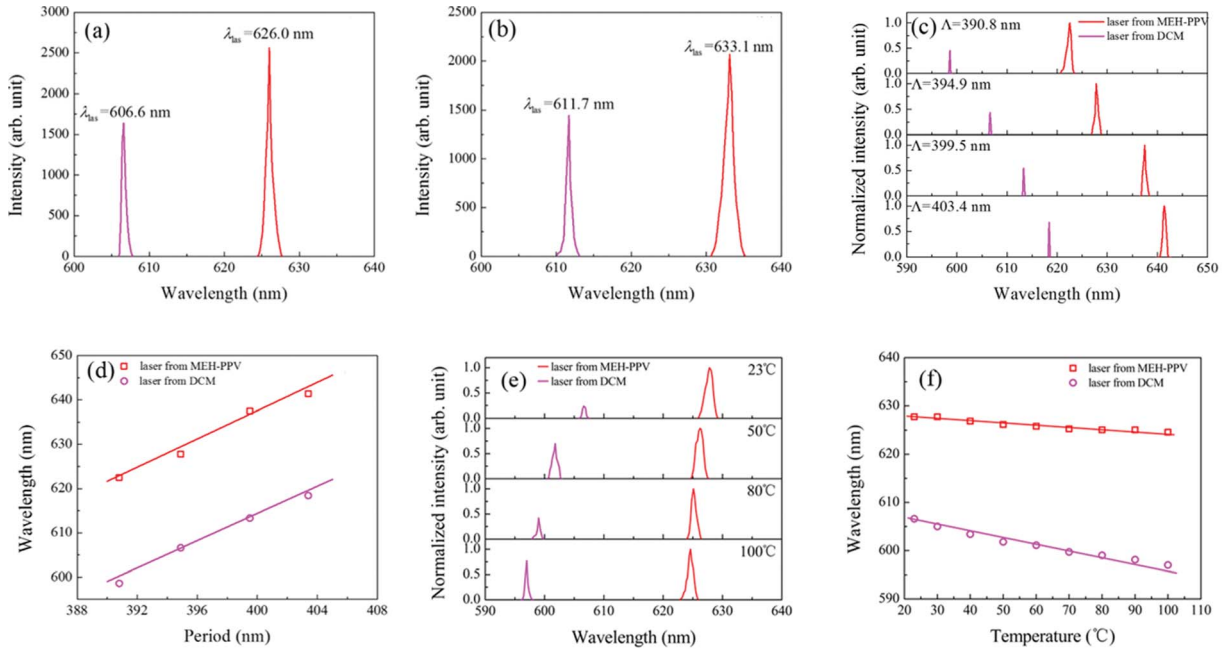

Fig. 5 Lasing spectra of (a) 2a with a thinner MEH-PPV layer (70 nm), (b) 3a with a higher average refractive index of the grating and (c) 1a, 4a–4c with different grating periods. (d) Lasing wavelengths as a function of the grating period. (e) Lasing spectra and (f) lasing wavelengths at different temperatures (1a).

shows that the output wavelength positions of the two lasers can be modulated individually. Therefore different gain materials or suitable structure parameters can realize more choices on the dual-wavelength lasing position modulations.

4. Conclusions

In conclusion, we have demonstrated an efficient dual-wavelength surface-emitting DFB laser from two organic gain materials in one laser beam based on holographic photopolymerization for the first time. The periodic DCM-doped HPDLC grating structure cured by a hologram between the glass and the MEH-PPV layer provides feedback for both laser gain materials. Two three-layer-structures, *i.e.*, grating/MEH-PPV/glass and glass/grating/MEH-PPV, form an asymmetric slab waveguide and a "leaky mode" slab waveguide, respectively. The two lasing actions from different working mechanisms are combined in one device. The spectral tunability of the dual-wavelength laser emission has been demonstrated by adjusting the structure parameters. Either dual lasing behaviors or single lasing behavior can be altered by different modulation methods. The results indicate that this designable dual-wavelength DFB laser can be exploited further for more practical applications.

Acknowledgements

The authors would like to thank the support from the National Natural Science Foundation of China (11174274, 11204299, 61377032 and 61378075).

References

1 (*a*) H. H. Telle, A. G. Urena and R. J. Donovan, *Laser Chemistry: Spectroscopy, Dynamics and Applications*, John Wiley & Sons, West Sussex, 2007; (*b*) W. M. Steen and J. Mazumder, *Lasers Material Processing*, Springer, London, 4th edn, 2010; (*c*) M. Maiwald, J. Fricke, A. Ginolas, J. Pohl, B. Sumpf, G. Erbert and G. Trankle, *Laser Photonics Rev.*, 2013, **7**, L30–L33.

2 F. J. Duarte, *Tunable Laser Applications*, CRC Press, New York, 2nd edn, 2009.

3 (*a*) N. Pavel, *Laser Phys.*, 2010, **20**, 215–221; (*b*) D. Sun, Y. Leng, Y. Sang, X. Kang, S. Liu, X. Qin, K. Cui, B. K. W. H. Anuar, H. Liu and Y. Bi, *CrystEngComm*, 2013, **15**, 7468–7474; (*c*) Y.-F. Chen, *Appl. Phys. B: Lasers Opt.*, 2000, **70**, 475–478; (*d*) L. Guo, R. Lan, H. Liu, H. Yu, H. Zhang, J. Wang, D. Hu, S. Zhuang, L. Chen and Y. Zhao, *Opt. Express*, 2010, **18**, 9098–9106.

4 (*a*) J. J. Coleman, A. C. Bryce and C. Jagadish, *Advances in Semiconductor Lasers*, Academic Press, London, 2012; (*b*) P. Pellandini, R. Stanley, R. Houdre, U. Oesterle, M. Ilegems and C. Weisbuch, *Appl. Phys. Lett.*, 1997, **71**, 864–866; (*c*) L. Fan, M. Fallahi, J. Hader, A. R. Zakharian, J. V. Moloney, W. Stolz, S. W. Koch, R. Bedford and J. T. Murray, *Appl. Phys. Lett.*, 2007, **90**, 181124.

5 C. Kallinger, M. Hilmer, A. Haugeneder, M. Perner, W. Spirkl, U. Lemmer, J. Feldmann, U. Scherf, K. Müllen and A. Gombert, *Adv. Mater.*, 1998, **10**, 920–923.

6 (*a*) F. Hide, M. A. Diaz-Garcia, B. J. Schwartz, M. R. Andersson, Q. Pei and A. J. Heeger, *Science*, 1996, **273**, 1833–1836; (*b*) B. J. Scott, G. Wirnsberger,

M. D. McGehee, B. F. Chmelka and G. D. Stucky, *Adv. Mater.*, 2001, **13**, 1231–1234.

7 Z. Diao, S. Deng, W. Huang, L. Xuan, L. Hu, Y. Liu and J. Ma, *J. Mater. Chem.*, 2012, **22**, 23331–23334.

8 (*a*) T. J. Bunning, L. V. Natarajan, V. P. Tondiglia and R. L. Sutherland, *Annu. Rev. Mater. Sci.*, 2000, **30**, 83–115; (*b*) R. Caputo, L. De Sio, A. Veltri, C. Umeton and A. V. Sukhov, *Opt. Lett.*, 2004, **29**, 1261–1263; (*c*) Y. J. Liu, H. T. Dai and X. W. Sun, *J. Mater. Chem.*, 2011, **21**, 2982–2986.

9 (*a*) L. De Sio, L. Ricciardi, S. Serak, M. La Deda, N. Tabiryan and C. Umeton, *J. Mater. Chem.*, 2012, **22**, 6669–6673; (*b*) L. De Sio, S. Serak, N. Tabiryan and T. Bunning, *J. Mater. Chem. C*, 2014, **2**, 3532–3535; (*c*) M. W. Jang and B. K. Kim, *J. Mater. Chem.*, 2011, **21**, 19226–19232; (*d*) V. K. S. Hsiao, K.-T. Yong, A. N. Cartwright, M. T. Swihart, P. N. Prasad, P. F. Lloyd and T. J. Bunning, *J. Mater. Chem.*, 2009, **19**, 3998–4003; (*e*) C. Y. Li, M. J. Birnkrant, L. V. Natarajan, V. P. Tondiglia, P. F. Lloyd, R. L. Sutherland and T. J. Bunning, *Soft Matter*, 2005, **1**, 238–242; (*f*) T. J. White, L. V. Natarajan, V. P. Tondiglia, P. F. Lloyd, T. J. Bunning and C. A. Guymon, *Polymer*, 2007, **48**, 5979–5987; (*g*) H. Kakiuchida, M. Tazawa, K. Yoshimura and A. Ogiwara, *Thin Solid Films*, 2014, DOI: 10.1016/j.tsf.2013.11.050.

10 W. Huang, Z. Diao, Y. Liu, Z. Peng, C. Yang, J. Ma and L. Xuan, *Org. Electron.*, 2012, **13**, 2307–2311.

11 (*a*) Z. Diao, W. Huang, Z. Peng, Q. Mu, Y. Liu, J. Ma and L. Xuan, *Liq. Cryst.*, 2014, **41**, 239–246; (*b*) W. Huang, Z. Diao, L. Yao, Z. Cao, Y. Liu, J. Ma and L. Xuan, *Appl. Phys. Express*, 2013, **6**, 022702; (*c*) W. Huang, Y. Liu, Z. Diao, C. Yang, L. Yao, J. Ma and L. Xuan, *Appl. Opt.*, 2012, **51**, 4013–4020; (*d*) J. Ma, L. Shi and D.-K. Yang, *Appl. Phys. Express*, 2010, **3**, 021702; (*e*) Z. Zheng, J. Song, Y. Liu, F. Guo, J. Ma and L. Xuan, *Liq. Cryst.*, 2008, **35**, 489–499.

12 (*a*) R. Jakubiak, T. J. Bunning, R. A. Vaia, L. V. Natarajan and V. P. Tondiglia, *Adv. Mater.*, 2003, **15**, 241–244; (*b*) R. Jakubiak, L. V. Natarajan, V. Tondiglia, G. S. He, P. N. Prasad, T. J. Bunning and R. A. Vaia, *Appl. Phys. Lett.*, 2004, **85**, 6095–6097; (*c*) R. Jakubiak, V. P. Tondiglia, L. V. Natarajan, R. L. Sutherland, P. Lloyd, T. J. Bunning and R. A. Vaia, *Adv. Mater.*, 2005, **17**, 2807–2811.

13 (*a*) O. Sakhno, J. Stumpe and T. Smirnova, *Appl. Phys. B: Lasers Opt.*, 2011, **103**, 907–916; (*b*) N. Tsutsumi and H. Nishida, *Opt. Commun.*, 2011, **284**, 3365–3368.

14 (*a*) I. D. W. Samuel and G. A. Turnbull, *Chem. Rev.*, 2007, **107**, 1272–1295; (*b*) W. Holzer, A. Penzkofer, T. Pertsch, N. Danz, A. Brauer, E. B. Kley, H. Tillmann, C. Bader and H.-H. Horhold, *Appl. Phys. B: Lasers Opt.*, 2002, **74**, 333–342.

15 H. Kogelnik and C. V. Shank, *J. Appl. Phys.*, 1972, **43**, 2327–2335.

16 M. Tammer and A. P. Monkman, *Adv. Mater.*, 2002, **14**, 210–212.

17 K. Okamoto, *Fundamentals of Optical Waveguides*, Academic Press, Burlington, 2nd edn, 2010.

18 T.-N. Ding and E. Garmire, *Appl. Opt.*, 1983, **22**, 3177–3181.

19 A. Costela, O. Garcia, L. Cerdan, I. Garcia-Moreno and R. Sastre, *Opt. Express*, 2008, **16**, 7023–7036.

20 M. Born and E. Wolf, *Principles of Optics: Electromagnetic Theory of Propagation, Interference and Diffraction of Light*, Cambridge University Press, New York, 1999.

21 G. Heliotis, R. Xia, G. A. Turnbull, P. Andrew, W. L. Barnes, I. D. Samuel and D. D. Bradley, *Adv. Funct. Mater.*, 2004, **14**, 91–97.

22 (*a*) J. Li, S. Gauza and S.-T. Wu, *J. Appl. Phys.*, 2004, **96**, 19–24; (*b*) X. Zhu and D. Lo, *J. Opt. A: Pure Appl. Opt.*, 2001, **3**, 225–228.

23 (*a*) D.-K. Yang and S.-T. Wu, *Fundamentals of Liquid Crystal Devices*, John Wiley & Sons Inc, New York, 2006; (*b*) J. Ma, Y. Li, T. White, A. Urbas and Q. Li, *Chem. Commun.*, 2010, **46**, 3463–3465; (*c*) J. Ma and L. Xuan, *Displays*, 2013, **34**, 293–300.

